



Observation of $B \rightarrow K^* \ell^+ \ell^-$

A. Ishikawa,²⁰ K. Abe,⁷ K. Abe,⁴¹ T. Abe,⁷ I. Adachi,⁷ Byoung Sup Ahn,¹⁴ H. Aihara,⁴³
K. Akai,⁷ M. Akatsu,²⁰ M. Akemoto,⁷ Y. Asano,⁴⁸ T. Aso,⁴⁷ V. Aulchenko,¹ T. Aushev,¹¹
A. M. Bakich,³⁸ Y. Ban,³¹ A. Bay,¹⁶ I. Bizjak,¹² A. Bondar,¹ A. Bozek,²⁵ M. Bračko,^{18,12}
T. E. Browder,⁶ P. Chang,²⁴ Y. Chao,²⁴ K.-F. Chen,²⁴ B. G. Cheon,³⁷ R. Chistov,¹¹
S.-K. Choi,⁵ Y. Choi,³⁷ Y. K. Choi,³⁷ A. Chuvikov,³² M. Danilov,¹¹ L. Y. Dong,⁹
A. Drutskoy,¹¹ S. Eidelman,¹ V. Eiges,¹¹ Y. Enari,²⁰ J. Flanagan,⁷ C. Fukunaga,⁴⁵
K. Furukawa,⁷ N. Gabyshev,⁷ A. Garmash,^{1,7} T. Gershon,⁷ B. Golob,^{17,12} R. Guo,²²
J. Haba,⁷ C. Hagner,⁵⁰ F. Handa,⁴² H. Hayashii,²¹ M. Hazumi,⁷ L. Hinz,¹⁶ T. Hokuue,²⁰
Y. Hoshi,⁴¹ W.-S. Hou,²⁴ Y. B. Hsiung,^{24,*} H.-C. Huang,²⁴ T. Iijima,²⁰ K. Inami,²⁰
R. Itoh,⁷ H. Iwasaki,⁷ M. Iwasaki,⁴³ Y. Iwasaki,⁷ J. H. Kang,⁵² J. S. Kang,¹⁴
N. Katayama,⁷ H. Kawai,² T. Kawasaki,²⁷ H. Kichimi,⁷ E. Kikutani,⁷ H. J. Kim,⁵²
Hyunwoo Kim,¹⁴ J. H. Kim,³⁷ S. K. Kim,³⁶ K. Kinoshita,³ P. Koppenburg,⁷ S. Korpar,^{18,12}
P. Križan,^{17,12} P. Krokovny,¹ A. Kuzmin,¹ Y.-J. Kwon,⁵² J. S. Lange,^{4,33} G. Leder,¹⁰
S. H. Lee,³⁶ T. Lesiak,²⁵ J. Li,³⁵ A. Limosani,¹⁹ S.-W. Lin,²⁴ D. Liventsev,¹¹
J. MacNaughton,¹⁰ G. Majumder,³⁹ F. Mandl,¹⁰ M. Masuzawa,⁷ T. Matsumoto,⁴⁵
A. Matyja,²⁵ S. Michizono,⁷ T. Mimashi,⁷ W. Mitaroff,¹⁰ K. Miyabayashi,²¹ H. Miyake,²⁹
H. Miyata,²⁷ D. Mohapatra,⁵⁰ T. Mori,⁴⁴ T. Nagamine,⁴² Y. Nagasaka,⁸ T. Nakadaira,⁴³
T. T. Nakamura,⁷ M. Nakao,⁷ H. Nakazawa,⁷ Z. Natkaniec,²⁵ S. Nishida,⁷ O. Nitoh,⁴⁶
T. Nozaki,⁷ S. Ogawa,⁴⁰ Y. Ogawa,⁷ K. Ohmi,⁷ Y. Ohnishi,⁷ T. Ohshima,²⁰ N. Ohuchi,⁷
T. Okabe,²⁰ S. Okuno,¹³ S. L. Olsen,⁶ W. Ostrowicz,²⁵ H. Ozaki,⁷ H. Palka,²⁵ C. W. Park,¹⁴
H. Park,¹⁵ N. Parslow,³⁸ L. S. Peak,³⁸ L. E. Piilonen,⁵⁰ N. Root,¹ H. Sagawa,⁷
S. Saitoh,⁷ Y. Sakai,⁷ T. R. Sarangi,⁴⁹ M. Satpathy,⁴⁹ A. Satpathy,^{7,3} O. Schneider,¹⁶
J. Schümann,²⁴ C. Schwanda,^{7,10} A. J. Schwartz,³ S. Semenov,¹¹ K. Senyo,²⁰
R. Seuster,⁶ M. E. Seviar,¹⁹ H. Shibuya,⁴⁰ T. Shidara,⁷ V. Sidorov,¹ J. B. Singh,³⁰
N. Soni,³⁰ S. Stanič,^{48,†} M. Starič,¹² A. Sugi,²⁰ A. Sugiyama,³⁴ K. Sumisawa,²⁹
T. Sumiyoshi,⁴⁵ S. Suzuki,⁵¹ S. Y. Suzuki,⁷ F. Takasaki,⁷ K. Tamai,⁷ N. Tamura,²⁷
M. Tanaka,⁷ M. Tawada,⁷ G. N. Taylor,¹⁹ Y. Teramoto,²⁸ T. Tomura,⁴³ T. Tsuboyama,⁷
T. Tsukamoto,⁷ S. Uehara,⁷ K. Ueno,²⁴ S. Uno,⁷ G. Varner,⁶ C. C. Wang,²⁴ C. H. Wang,²³
J. G. Wang,⁵⁰ M.-Z. Wang,²⁴ Y. Watanabe,⁴⁴ E. Won,¹⁴ B. D. Yabsley,⁵⁰ Y. Yamada,⁷
A. Yamaguchi,⁴² Y. Yamashita,²⁶ M. Yamauchi,⁷ H. Yanai,²⁷ Heyoung Yang,³⁶
J. Ying,³¹ M. Yoshida,⁷ Y. Yusa,⁴² Z. P. Zhang,³⁵ V. Zhilich,¹ and D. Žontar^{17,12}

(The Belle Collaboration)

¹*Budker Institute of Nuclear Physics, Novosibirsk*

²*Chiba University, Chiba*

³*University of Cincinnati, Cincinnati, Ohio 45221*

⁴*University of Frankfurt, Frankfurt*

- ⁵Gyeongsang National University, Chinju
⁶University of Hawaii, Honolulu, Hawaii 96822
⁷High Energy Accelerator Research Organization (KEK), Tsukuba
⁸Hiroshima Institute of Technology, Hiroshima
⁹Institute of High Energy Physics, Chinese Academy of Sciences, Beijing
¹⁰Institute of High Energy Physics, Vienna
¹¹Institute for Theoretical and Experimental Physics, Moscow
¹²J. Stefan Institute, Ljubljana
¹³Kanagawa University, Yokohama
¹⁴Korea University, Seoul
¹⁵Kyungpook National University, Taegu
¹⁶Institut de Physique des Hautes Énergies, Université de Lausanne, Lausanne
¹⁷University of Ljubljana, Ljubljana
¹⁸University of Maribor, Maribor
¹⁹University of Melbourne, Victoria
²⁰Nagoya University, Nagoya
²¹Nara Women's University, Nara
²²National Kaohsiung Normal University, Kaohsiung
²³National Lien-Ho Institute of Technology, Miao Li
²⁴Department of Physics, National Taiwan University, Taipei
²⁵H. Niewodniczanski Institute of Nuclear Physics, Krakow
²⁶Nihon Dental College, Niigata
²⁷Niigata University, Niigata
²⁸Osaka City University, Osaka
²⁹Osaka University, Osaka
³⁰Panjab University, Chandigarh
³¹Peking University, Beijing
³²Princeton University, Princeton, New Jersey 08545
³³RIKEN BNL Research Center, Upton, New York 11973
³⁴Saga University, Saga
³⁵University of Science and Technology of China, Hefei
³⁶Seoul National University, Seoul
³⁷Sungkyunkwan University, Suwon
³⁸University of Sydney, Sydney NSW
³⁹Tata Institute of Fundamental Research, Bombay
⁴⁰Toho University, Funabashi
⁴¹Tohoku Gakuin University, Tagajo
⁴²Tohoku University, Sendai
⁴³Department of Physics, University of Tokyo, Tokyo
⁴⁴Tokyo Institute of Technology, Tokyo
⁴⁵Tokyo Metropolitan University, Tokyo
⁴⁶Tokyo University of Agriculture and Technology, Tokyo
⁴⁷Toyama National College of Maritime Technology, Toyama
⁴⁸University of Tsukuba, Tsukuba
⁴⁹Utkal University, Bhubaneswer
⁵⁰Virginia Polytechnic Institute and State University, Blacksburg, Virginia 24061
⁵¹Yokkaichi University, Yokkaichi

⁵²*Yonsei University, Seoul*
(Dated: September 12, 2003)

Abstract

We report the first observation of the flavor-changing neutral current decay $B \rightarrow K^* \ell^+ \ell^-$ and an improved measurement of the decay $B \rightarrow K \ell^+ \ell^-$, where ℓ represents an electron or a muon, with a data sample of 140 fb^{-1} accumulated at the $\Upsilon(4S)$ resonance with the Belle detector at KEKB. The results for the branching fractions are $\mathcal{B}(B \rightarrow K^* \ell^+ \ell^-) = (11.5_{-2.4}^{+2.6} \pm 0.8 \pm 0.2) \times 10^{-7}$ and $\mathcal{B}(B \rightarrow K \ell^+ \ell^-) = (4.8_{-0.9}^{+1.0} \pm 0.3 \pm 0.1) \times 10^{-7}$, where the first error is statistical, the second is systematic and the third is from model dependence.

PACS numbers: 11.30.Hv, 13.20.He, 14.65.Fy, 14.40.Nd

Flavor-changing neutral current (FCNC) processes are forbidden at tree level in the Standard Model (SM); they only proceed at a low rate via higher-order loop diagrams. SM decay amplitudes for the FCNC processes $B \rightarrow X_s \gamma$ and $B \rightarrow X_s \ell^+ \ell^-$, where X_s denotes inclusive hadronic final states with a strangeness $S = \pm 1$ and ℓ represents an electron or a muon, have been calculated with small errors [1]. If additional diagrams with non-SM particles contribute to these FCNC processes, their amplitudes will interfere with the SM amplitudes, making these processes ideal places to search for new physics [2].

Measurements of the decay rate for $B \rightarrow X_s \gamma$ [3] as well as the recent first exclusive and inclusive measurements by Belle for $B \rightarrow K \ell^+ \ell^-$ [4] and $B \rightarrow X_s \ell^+ \ell^-$ [5] have so far shown no disagreement with the SM predictions. Deviations due to non-SM amplitudes are often expressed in terms of the Wilson coefficients C_7 , C_9 and C_{10} ; a strong constraint on the magnitude of C_7 has been set by $B \rightarrow X_s \gamma$, and a large area of the C_9 – C_{10} plane has been excluded by $B \rightarrow K \ell^+ \ell^-$ and $B \rightarrow X_s \ell^+ \ell^-$ [6]. A complete determination of all three Wilson coefficients, including the sign of C_7 , requires the measurement of the forward-backward asymmetry in $B \rightarrow K^* \ell^+ \ell^-$ or $B \rightarrow X_s \ell^+ \ell^-$; however, $B \rightarrow K^* \ell^+ \ell^-$ has not been previously observed.

In this Letter, we report the first observation of the decay $B \rightarrow K^* \ell^+ \ell^-$, using a data sample of 152 million B meson pairs, corresponding to 140 fb^{-1} taken at the $\Upsilon(4S)$ resonance. We also report an improved measurement of $B \rightarrow K \ell^+ \ell^-$, superseding our previous result based on 29 fb^{-1} [4].

The data are produced in e^+e^- annihilation at the KEKB energy-asymmetric (3.5 on 8 GeV) collider [7] and collected with the Belle detector [8]. The Belle detector is a large-solid-angle spectrometer that includes a three-layer silicon vertex detector (SVD), a 50-layer central drift chamber (CDC), an array of aerogel threshold Cherenkov counters (ACC), time-of-flight (TOF) scintillation counters, and an electromagnetic calorimeter (ECL) comprised of CsI(Tl) crystals located inside a superconducting solenoid coil that provides a 1.5 T magnetic field. An iron flux-return located outside of the coil is instrumented to identify muons (KLM).

The event reconstruction procedure is similar to our previous report [4]. We reconstruct the following final states: $B^0 \rightarrow K^{*0} \ell^+ \ell^-$, $B^+ \rightarrow K^{*+} \ell^+ \ell^-$, $B^0 \rightarrow K_S^0 \ell^+ \ell^-$ and $B^+ \rightarrow K^+ \ell^+ \ell^-$. Charge conjugate modes are implied throughout this Letter. The following decay chains are used to reconstruct the intermediate states: $K^{*0} \rightarrow K^+ \pi^-$, $K^{*+} \rightarrow K_S^0 \pi^+$ and $K^{*+} \rightarrow K^+ \pi^0$, $K_S^0 \rightarrow \pi^+ \pi^-$, and $\pi^0 \rightarrow \gamma \gamma$.

Charged tracks are classified as e , μ , K and π candidates by discriminating between the flavors for the pairwise combinations, using criteria which allow multiple classifications of an individual track. The e/h discriminant (where $h = K$ or π) is formed from the energy deposit in the ECL, the specific ionization measurements in the CDC, and the ACC light yield. The μ/h discriminant is based on the hits in the KLM. The K/π and K/μ discriminants use the CDC, ACC, and TOF information. Electrons, muons and kaons are selected using loose conditions on the e/h , μ/h and K/π discriminants, respectively. All tracks are classified as pions unless they satisfy tight conditions on e/h or K/π ; the same e/h condition is required for kaons, and a similar K/μ condition is required for muons. To reduce the misidentification of hadrons as leptons, we require minimum momenta of $0.4 \text{ GeV}/c$ and $0.7 \text{ GeV}/c$ for electrons and muons, respectively. We apply a tight requirement for the muons below $1.0 \text{ GeV}/c$. Each of the charged tracks, except for the $K_S^0 \rightarrow \pi^+ \pi^-$ daughters, is required to have an impact parameter with respect to the interaction point of less than 0.5 cm transverse to, and 5.0 cm along the positron beam axis. Photons are reconstructed

within the ECL with a minimum energy requirement of 50 MeV.

Invariant masses for the π^0 , K_S^0 and K^{*} candidates are required to be within windows of ± 10 MeV/ c^2 ($\sim 2\sigma$), ± 15 MeV/ c^2 ($\sim 3.3\sigma$) and ± 75 MeV/ c^2 (1.5Γ), respectively, around their nominal masses. We require a minimum momentum of 0.1 GeV/ c for the π^0 candidates. We impose K_S^0 selection criteria based on the distance and the direction of the K_S^0 vertex and the impact parameters of daughter tracks. For $K^{*+} \rightarrow K^+\pi^0$, $\cos\theta_{\text{hel}} < 0.8$ is required to reduce background from soft π^0 s, where θ_{hel} is the angle between the K^{*+} momentum in the B rest frame and the K^+ momentum in the K^{*+} rest frame.

We form B candidates by combining a $K^{(*)}$ candidate and an oppositely charged lepton pair using two variables: the beam-energy constrained mass $M_{\text{bc}} = \sqrt{(E_{\text{beam}}^*/c^2)^2 - |p_B^*/c|^2}$ and the energy difference $\Delta E = E_B^* - E_{\text{beam}}^*$, where p_B^* and E_B^* are the measured momentum and energy, respectively, of the B candidate, and E_{beam}^* is the beam energy. Here and throughout this Letter, variables denoted with an asterisk are calculated in the $\Upsilon(4S)$ rest frame. When multiple candidates are found in an event, we select the candidate with the smallest value of $|\Delta E|$.

The following five types of backgrounds are considered. 1) *Charmonium* B decay background from $B \rightarrow J/\psi X_s$ and $B \rightarrow \psi' X_s$ decays is removed by vetoing lepton pairs whose invariant mass ($M_{\ell\ell}$) is near the J/ψ or ψ' mass [4]. In addition, we reject events that have a photon with energy less than 500 MeV within a 50 mrad cone around either the electron or positron direction (or a photon within each cone) and an $e^+e^-\gamma(\gamma)$ invariant mass within the veto windows. For $K^*\ell^+\ell^-$ modes, we reject the event if an unobserved photon along one of the lepton directions with an energy $E_{\text{beam}}^* - E_K^* - E_{\ell\ell}^*$ can replace the pion, giving $M_{\ell\ell\gamma}$ and M_{bc} consistent with $B \rightarrow J/\psi K$. 2) We suppress background from *photon conversions* and $\pi^0 \rightarrow e^+e^-\gamma$ by requiring the dielectron mass to satisfy $M_{ee} > 0.14$ GeV/ c^2 . This eliminates possible background from $B \rightarrow K^*\gamma$ and $B \rightarrow K^{(*)}\pi^0$. 3) Background from *continuum* $q\bar{q}$ ($q = u, d, s, c$) production is suppressed using a likelihood ratio $\mathcal{R}_{\text{cont}}$ formed from a Fisher discriminant, $\cos\theta_B^*$, and, for $K^{(*)}e^+e^-$ only, $\cos\theta_{\text{sph}}^*$. The Fisher discriminant [9] is calculated from the energy flow in 9 cones along the B candidate sphericity axis and the normalized second Fox-Wolfram moment R_2 [10]. The angles θ_B^* and θ_{sph}^* are the B meson angles with respect to the beam and the sphericity axes, respectively. 4) *Semileptonic* B decay background is suppressed using another likelihood ratio \mathcal{R}_{sl} , formed from the missing energy of the event, E_{miss}^* , and $\cos\theta_B^*$. 5) *Hadronic* B decay background, $B \rightarrow K^{(*)}h^+h^-$, e.g., from $B \rightarrow D\pi$, can contribute if two hadrons are misidentified as leptons. We find that other potential backgrounds are negligible.

For each decay mode, the selection criteria on the two likelihood ratios $\mathcal{R}_{\text{cont}}$ and \mathcal{R}_{sl} are chosen to maximize $N_S/\sqrt{N_S + N_B}$, where N_S is the expected signal yield and N_B is the expected background in the M_{bc} and ΔE signal windows. The signal windows ($\sim 2.5\sigma$) are defined as $|M_{\text{bc}} - M_B| < 0.007$ GeV/ c^2 for both lepton modes and $-0.055(-0.035)$ GeV $< \Delta E < 0.035$ GeV for the electron (muon) mode. A large Monte Carlo (MC) background sample of a mixture of $b \rightarrow c$ decays and $e^+e^- \rightarrow q\bar{q}$ events is used to estimate N_B . The $B \rightarrow K^{(*)}\ell^+\ell^-$ signal events are generated according to Ref. [6] to determine N_S , and to estimate the efficiencies that are summarized in Table I.

The signal yield is determined by a binned maximum-likelihood fit to the M_{bc} distribution for the events within the ΔE signal window using a Gaussian signal plus three background functions. The area of this Gaussian function is the signal yield; the mean and width are determined using observed $J/\psi K^{(*)}$ events. We find no dilepton mass dependence of the width and mean using a MC study. The first background function is for the semileptonic B

decays and, to a lesser extent, the continuum background, and is modeled with a threshold function [11] whose shape parameter is determined using a large MC sample that contains oppositely charged leptons and whose normalization is allowed to float. This MC sample reproduces the background parametrization for $B \rightarrow K^{(*)}e^{\pm}\mu^{\mp}$ data in which only combinatorial background is expected. The two other background functions account for the residual B to charmonium decays and hadronic B decays, and are modeled with separate combinations of a similar threshold function and an additional Gaussian component. The shape and the size of the charmonium background function are fixed from J/ψ and ψ' inclusive MC samples. We find the Gaussian component of the charmonium background contributes less than one event. The shape and the size of the hadronic background are evaluated using hadron enriched data by relaxing the lepton identification criteria. The Gaussian components of the hadronic background contribution, multiplied by the lepton misidentification probability (measured in bins of momentum and polar angle with respect to the positron beam), are then found to be 1.05 ± 0.08 and 0.64 ± 0.05 events for $B \rightarrow K\ell^+\ell^-$ and $B \rightarrow K^*\ell^+\ell^-$, respectively.

Figure 1 and Table I give the fit results. We observe $35.8_{-7.3}^{+8.0}(\text{stat.}) \pm 1.7(\text{syst.})$ $B \rightarrow K^*\ell^+\ell^-$ signal events with a significance of 5.7, and $37.9_{-6.9}^{+7.6}(\text{stat.})_{-1.1}^{+1.0}(\text{syst.})$ $B \rightarrow K\ell^+\ell^-$ signal events with a significance of 7.4. The error due to uncertainty in the fixed parameters is included in the systematic error. To evaluate the uncertainty in the signal function parametrization, the mean and width of the Gaussian function are changed by ± 1 standard deviation (σ) from the values determined from $J/\psi K^{(*)}$ events. The uncertainty in the semileptonic plus continuum background parametrization, which is the largest error source, is obtained by varying the parameter by $\pm 1\sigma$ from the value determined with a large MC sample. The uncertainties of the hadronic (charmonium) background contributions are evaluated by changing the shape parameters and the normalizations of the Gaussian and threshold components by $\pm 1\sigma$ ($\pm 100\%$). The significance is defined as $\sqrt{-2 \ln(\mathcal{L}_0/\mathcal{L}_{\max})}$, where \mathcal{L}_{\max} is the maximum likelihood in the M_{bc} fit and \mathcal{L}_0 is the likelihood of the best fit when the signal yield is constrained to be zero. In order to include the effect of systematic error in the significance calculation, we use the parameters simultaneously changed by 1σ (100% for the charmonium background) in the direction that reduces the resulting significance.

In addition to the systematic error in the signal yield, we consider the following experimental systematic errors in the efficiency determination. For each charged track, we estimate the systematic error due to reconstruction efficiency to be 1.0%, and the systematic errors due to kaon, pion, electron and muon identification to be 1.0%, 0.8%, 0.5% and 1.2%, respectively. For each K_S^0 candidate and π^0 candidate, we estimate the systematic errors due to reconstruction efficiencies to be 4.5% and 2.7%, respectively. The uncertainty in the background suppression is estimated to be 2.3% using $J/\psi K^{(*)}$ control samples. Systematic errors due to MC statistics range from 0.5% to 2.2%. All these errors are added in quadrature.

The uncertainty due to the theoretical model assumptions is evaluated by calculating the efficiency for signal MC samples generated using three form-factor models [6, 12] and taking the maximum difference as the model-dependence error.

When calculating the branching fractions, we assume an equal production rate for charged and neutral B meson pairs, isospin invariance, lepton universality for $B \rightarrow K\ell^+\ell^-$, and the branching ratio $\mathcal{B}(B \rightarrow K^*e^+e^-)/\mathcal{B}(B \rightarrow K^*\mu^+\mu^-) = 1.33$ [6]. The combined efficiency and

branching fraction are scaled to the muon mode. We find

$$\begin{aligned}\mathcal{B}(B \rightarrow K^*\ell^+\ell^-) &= (11.5_{-2.4}^{+2.6} \pm 0.8 \pm 0.2) \times 10^{-7}, \\ \mathcal{B}(B \rightarrow K\ell^+\ell^-) &= (4.8_{-0.9}^{+1.0} \pm 0.3 \pm 0.1) \times 10^{-7},\end{aligned}$$

where the first error is statistical, the second is systematic, and the third is from model dependence. This systematic error is a quadratic sum of the systematic errors in the yield and efficiency, and the uncertainty in B meson pair counting of 0.5 %. The results are consistent with the SM predictions [6, 12, 13], our previous values [4], and results recently reported by BaBar [14]. The complete set of results is given in Table I.

For the modes with a significance of less than 3, we set 90% confidence level upper limits. The upper limit on the yield, N , is defined as $\int_0^N \mathcal{L}(n)dn = 0.9 \int_0^\infty \mathcal{L}(n)dn$. The function $\mathcal{L}(n)$ is the likelihood for signal yield n , using signal and background shape parameters that are modified by 1σ of their errors in the direction to increase the signal yield. The upper limits for the branching fractions are then calculated by using the efficiencies reduced by 1σ of their errors.

Figure 2 shows the measured $q^2 = M_{\ell\ell}^2 c^2$ distributions for $B \rightarrow K\ell^+\ell^-$ and $K^*\ell^+\ell^-$. The signal yield is extracted in each q^2 bin from a fit to the M_{bc} distributions.

In summary, we have observed the decay $B \rightarrow K^*\ell^+\ell^-$ for the first time. This mode will provide a useful sample for a forward-backward asymmetry measurement. The $B \rightarrow K\ell^+\ell^-$ decay is also measured with improved accuracy. The measured branching fractions are in agreement with the SM predictions, and may be used to provide more stringent constraints on physics beyond the SM.

We wish to thank the KEKB accelerator group for the excellent operation of the KEKB accelerator. We acknowledge support from the Ministry of Education, Culture, Sports, Science, and Technology of Japan and the Japan Society for the Promotion of Science; the Australian Research Council and the Australian Department of Education, Science and Training; the National Science Foundation of China under contract No. 10175071; the Department of Science and Technology of India; the BK21 program of the Ministry of Education of Korea and the CHEP SRC program of the Korea Science and Engineering Foundation; the Polish State Committee for Scientific Research under contract No. 2P03B 01324; the Ministry of Science and Technology of the Russian Federation; the Ministry of Education, Science and Sport of the Republic of Slovenia; the National Science Council and the Ministry of Education of Taiwan; and the U.S. Department of Energy.

* on leave from Fermi National Accelerator Laboratory, Batavia, Illinois 60510

† on leave from Nova Gorica Polytechnic, Nova Gorica

- [1] P. Gambino and M. Misiak, Nucl. Phys. B **611**, 338 (2001) and references therein; C. Bobeth, M. Misiak and J. Urban, Nucl. Phys. B **567**, 153 (2000); H. H. Asatrian, H. M. Asatrian, C. Greub and M. Walker, Phys. Lett. B **507**, 162 (2001).
- [2] For example, E. Lunghi, A. Masiero, I. Scimemi and L. Silverstrini, Nucl. Phys. B **568**, 120 (2000); J. L. Hewett and J. D. Wells, Phys. Rev. D **55**, 5549 (1997); T. Goto, Y. Okada, Y. Shimizu and M. Tanaka, Phys. Rev. D **55**, 4273 (1997); G. Burdman, Phys. Rev. D **52**, 6400 (1995); N. G. Deshpande, K. Panose and J. Trampetić, Phys. Lett. B **308**, 322 (1993); W. S. Hou, R. S. Willey and A. Soni, Phys. Rev. Lett. **58**, 1608 (1987).

TABLE I: Summary of the results: signal yields obtained from the M_{bc} fit and their significances, reconstruction efficiencies including the intermediate branching fractions, branching fractions (\mathcal{B}) and their 90% confidence level upper limits.

Mode	Signal yield $\pm\text{stat.}\pm\text{syst.}$	Significance	Efficiency [%] $\pm\text{syst.}\pm\text{model}$	$\mathcal{B} [\times 10^{-7}]$ $\pm\text{stat.}\pm\text{syst.}\pm\text{model}$	Upper Limit [$\times 10^{-7}$]
$K^{*0}e^+e^-$	$10.2^{+4.5}_{-3.8} \pm 0.8$	2.8	$5.2 \pm 0.3 \pm 0.04$	$12.9^{+5.7}_{-4.9} \pm 1.1 \pm 0.1$	24
$K^{*+}e^+e^-$	$5.3^{+3.3+0.5}_{-2.6-0.6}$	1.9	$1.7 \pm 0.1 \pm 0.1$	$20.2^{+12.7+2.3}_{-10.1-2.4} \pm 0.7$	46
$K^*e^+e^-$	$15.6^{+5.5}_{-4.8} \pm 1.0$	3.5	$3.5 \pm 0.2 \pm 0.04$	$14.9^{+5.2+1.2}_{-4.6-1.3} \pm 0.2$	—
$K^0e^+e^-$	$0.0^{+1.5+0.2}_{-0.9-0.3}$	0.0	$5.0 \pm 0.3 \pm 0.1$	$0.0^{+2.0+0.3}_{-1.2-0.4} \pm 0.0$	5.4
$K^+e^+e^-$	$15.9^{+4.9}_{-4.2} \pm 0.6$	5.1	$16.6 \pm 0.7 \pm 0.4$	$6.3^{+1.9}_{-1.7} \pm 0.3 \pm 0.1$	—
Ke^+e^-	$15.9^{+5.1}_{-4.4} \pm 0.7$	4.5	$10.8 \pm 0.5 \pm 0.2$	$4.8^{+1.5}_{-1.3} \pm 0.3 \pm 0.1$	—
$K^{*0}\mu^+\mu^-$	$17.1^{+5.4}_{-4.7} \pm 0.9$	4.2	$8.5 \pm 0.5 \pm 0.3$	$13.3^{+4.2}_{-3.7} \pm 1.0 \pm 0.5$	—
$K^{*+}\mu^+\mu^-$	$2.8^{+2.9}_{-2.3} \pm 0.6$	0.8	$2.8 \pm 0.2 \pm 0.2$	$6.5^{+6.9+1.4}_{-5.3-1.5} \pm 0.4$	22
$K^*\mu^+\mu^-$	$20.0^{+6.0+1.1}_{-5.3-1.2}$	4.2	$5.6 \pm 0.3 \pm 0.2$	$11.7^{+3.6}_{-3.1} \pm 0.9 \pm 0.5$	—
$K^0\mu^+\mu^-$	$5.7^{+3.0+0.2}_{-2.3-0.3}$	3.1	$6.7 \pm 0.4 \pm 0.3$	$5.6^{+2.9}_{-2.3} \pm 0.4 \pm 0.3$	—
$K^+\mu^+\mu^-$	$16.3^{+5.1+0.7}_{-4.5-0.8}$	4.6	$23.6 \pm 1.1 \pm 0.6$	$4.5^{+1.4}_{-1.2} \pm 0.3 \pm 0.1$	—
$K\mu^+\mu^-$	$22.0^{+5.8}_{-5.1} \pm 0.8$	5.6	$15.2 \pm 0.7 \pm 0.5$	$4.8^{+1.2}_{-1.1} \pm 0.3 \pm 0.2$	—
$K^{*0}\ell^+\ell^-$	$27.4^{+6.9}_{-6.2} \pm 1.3$	5.2	$7.7 \pm 0.4 \pm 0.2$	$11.7^{+3.0}_{-2.7} \pm 0.8 \pm 0.3$	—
$K^{*+}\ell^+\ell^-$	$8.1^{+4.3+0.8}_{-3.3-0.9}$	2.1	$2.5 \pm 0.2 \pm 0.05$	$10.5^{+5.6+1.2}_{-4.3-1.1} \pm 0.2$	22
$K^*\ell^+\ell^-$	$35.8^{+8.0}_{-7.3} \pm 1.7$	5.7	$5.1 \pm 0.3 \pm 0.1$	$11.5^{+2.6}_{-2.4} \pm 0.8 \pm 0.2$	—
$K^0\ell^+\ell^-$	$5.7^{+3.4+0.4}_{-2.7-0.5}$	2.3	$5.9 \pm 0.4 \pm 0.2$	$3.2^{+1.9}_{-1.5} \pm 0.3 \pm 0.1$	6.8
$K^+\ell^+\ell^-$	$32.3^{+6.9+0.9}_{-6.2-1.0}$	7.0	$20.1 \pm 0.9 \pm 0.1$	$5.3^{+1.1}_{-1.0} \pm 0.3 \pm 0.04$	—
$K\ell^+\ell^-$	$37.9^{+7.6+1.0}_{-6.9-1.1}$	7.4	$13.0 \pm 0.6 \pm 0.2$	$4.8^{+1.0}_{-0.9} \pm 0.3 \pm 0.1$	—

- [3] Belle Collaboration, K. Abe *et al.*, Phys. Lett. B **511**, 151 (2001); CLEO Collaboration, S. Chen *et al.*, Phys. Rev. Lett. **87**, 251807 (2001); ALEPH Collaboration, R. Barate *et al.*, Phys. Lett. B **429**, 169 (1998).
- [4] Belle Collaboration, K. Abe *et al.*, Phys. Rev. Lett. **88**, 021801 (2002); A. Ishikawa, Ph.D. thesis (Nagoya Univ., Mar. 2002), <http://belle.kek.jp/bdocs/theses.html>.
- [5] Belle Collaboration, J. Kaneko *et al.*, Phys. Rev. Lett. **90**, 021801 (2003).
- [6] A. Ali, E. Lunghi, C. Greub and G. Hiller, Phys. Rev. D **66**, 034002 (2002); E. Lunghi, arXiv:hep-ph/0210379.
- [7] S. Kurokawa and E. Kikutani, Nucl. Instrum. Meth. A **499**, 1 (2003), and other papers included in this Volume.
- [8] Belle Collaboration, A. Abashian *et al.*, Nucl. Instrum. Meth. A **479**, 117 (2002).
- [9] R. A. Fisher, Ann. Eugen. **7**, 179 (1936).
- [10] G. C. Fox and S. Wolfram, Phys. Rev. Lett. **41**, 1581 (1978).
- [11] ARGUS Collaboration, H. Albrecht *et al.*, Phys. Lett. B **241**, 278 (1990).
- [12] D. Melikhov, N. Nikitin and S. Simula, Phys. Lett. B **410**, 290 (1997); P. Colangelo, F. De Fazio, P. Santorelli and E. Scrimieri, Phys. Rev. D **53**, 3672 (1996), Erratum-ibid. D **57**, 3186 (1998).
- [13] For example, M. Zhong, Y. L. Wu and W. Y. Wang, Int. J. Mod. Phys. A **18**, 1959 (2003);

- A. Faessler *et al.*, Eur. Phys. J. direct C **4**, 18 (2002); T. M. Aliev, C. S. Kim and Y. G. Kim, Phys. Rev. D **62**, 014026 (2000); W. Jaus and D. Wyler, Phys. Rev. D **41**, 3405 (1990).
- [14] BaBar Collaboration, B. Aubert *et al.*, arXiv:hep-ex/0308042.

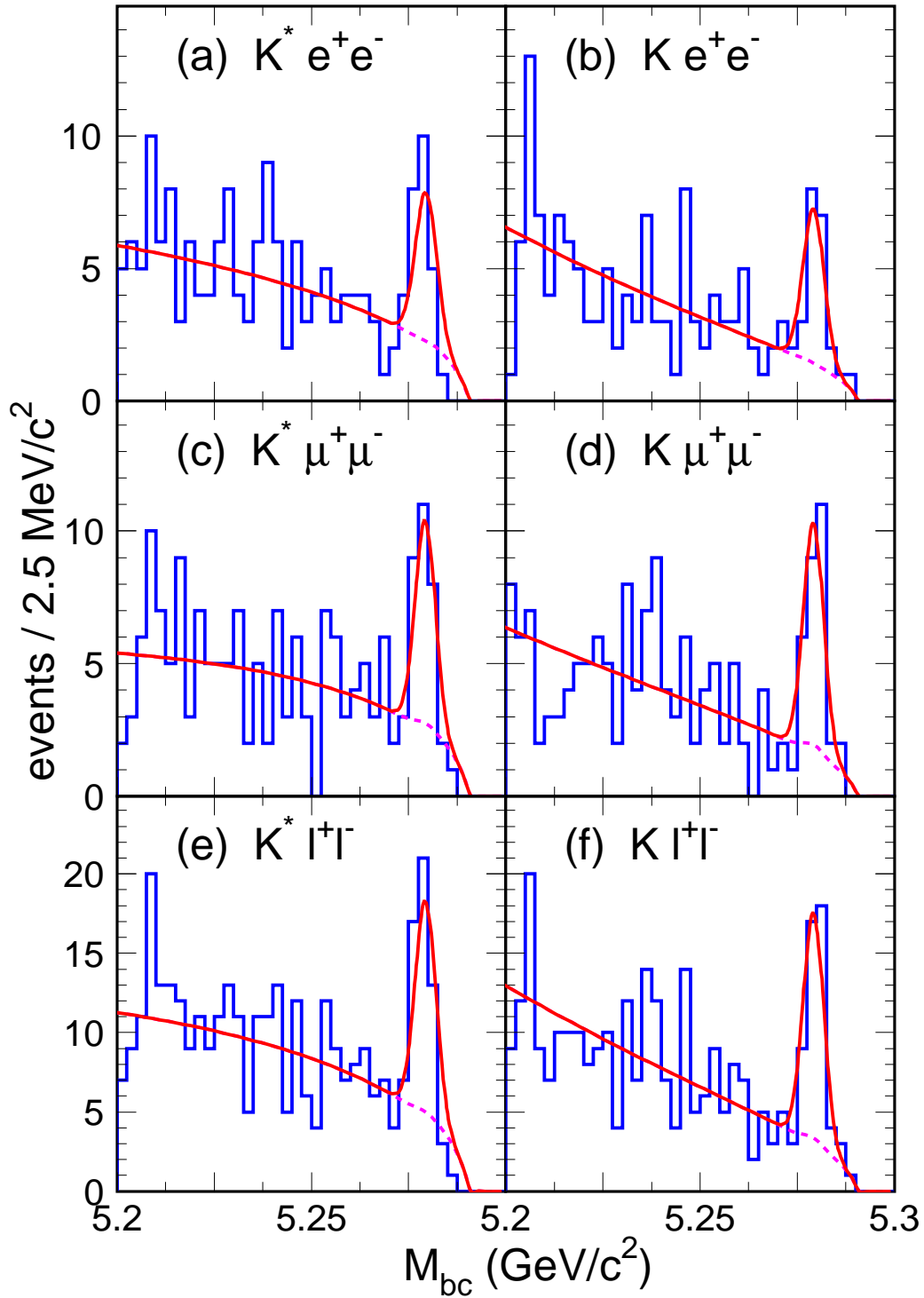


FIG. 1: M_{bc} distributions (histograms) for $K^{(*)}\ell^+\ell^-$ samples. Solid and dotted curves show the results of the fits and the background contributions, respectively.

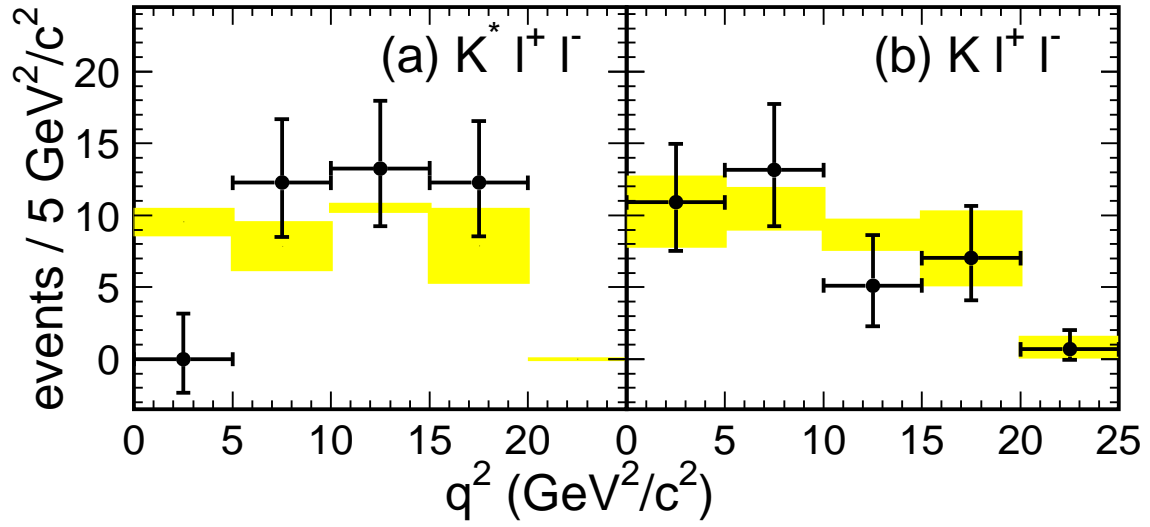


FIG. 2: q^2 distributions of (a) $K^* \ell^+ \ell^-$ and (b) $K \ell^+ \ell^-$. Points with error bars show the data while the hatched boxes show the range of SM expectations from various models [6, 12]. Statistical and systematic errors are added in quadrature.